Int. J. Heat Mass Transfer. Vol. 32, No. 3, pp. 595–609, 1989
Printed in Great Britain

0017–9310/89 $3.00+0.00

The effective thermal conductivity of high temperature particulate beds—II. Model predictions and the implication of the experimental values

J. S. M. BOTTERILL, A. G. SALWAY† and Y. TEOMAN‡

Department of Chemical Engineering, University of Birmingham, P.O. Box 363, Birmingham B15 2TT, U.K.

(*Received* 12 *November* 1987 *and in final form* 16 *August* 1988)

Abstract—A range of the published models, both unit cell and pseudohomogeneous chosen to illustrate the different approaches to modelling effective thermal conductivity, are reviewed. Their predictions are compared with experimental values obtained for packed beds of alumina and sand within the temperature range from 400 to 950°C. None predicts the high degree of temperature dependence observed. Their inadequacy is attributed to the assumption that the particles are opaque to radiation whereas both alumina and silica are partially transmissive. Deficiencies in the prediction of the conductive component by some models is attributed to their inability to characterize the effects of particle shape and size distribution. The Godbee and Ziegler (*J. Appl. Phys.* **37,** 55 (1966)) and Kunii and Smith (*A.I.Ch.E. Jl* **6,** 71 (1960)) models gave reasonable predictions for the conductive component of the silica beds at the lower temperatures for which radiant transfer is negligible.

1. INTRODUCTION

PART I of this paper reports measured effective thermal conductivities of packed beds of sand and alumina at temperatures up to 950°C. A very strong temperature dependence was found and the implications of this is discussed in relation to the predictions of a range of models for static bed conductivities. It is notable that although the models, which are briefly reviewed, differ markedly between themselves, they all give predictions within a factor of two of each other but none predicts the degree of temperature dependence found.

2. PACKED BED HEAT TRANSFER MODELS

Precise prediction of the effective thermal conductivity of a granular bed would require a knowledge of the shape, size, location and conductivity of each particle and their interaction. This is difficult for a regular array of particles and generally not feasible for a randomly packed bed so the usual approach to the problem has been to represent the bed or part of it by a geometrically simplified unit cell and to calculate the conductivity of this representative unit. However, the conductivity of the unit cell may only approximate to that of the bed and the unit cell approach cannot take into account the long range effect of radiation. When allowance needs to be made for these, resort is made to pseudohomogeneous models.

2.1. *The Wakao and Kato* [1] *model*

Wakao and Kato [1] calculated the effective thermal conductivity of an orthorhombic array of uniform spheres ($\varepsilon = 0.395$) using a relaxation technique and allowing for three-dimensional heat transfer, a finite contact area between adjacent spheres and radiation. The problem was simplified to the calculation of the profile around a single sphere. Radiant transfer was assumed to take place in one dimension between adjacent solid surfaces and also between void surfaces within the unit cell. By considering the view factors between these surfaces they evaluated an overall radiant heat transfer coefficient which was then incorporated in the relaxation network. They also performed calculations for a cubic array ($\varepsilon = 0.476$) and obtained good agreement with the earlier calculations of Deissler and Boegli [2]. Wakao and Vortmeyer [3] have extended this model to take account of low pressure conditions causing a reduction in the thermal conductivity of the gas in the voids.

2.2. *The Imura and Takegoshi* [4] *model*

This model is a variant of a number of unit cell models, namely those of Yagi and Kunii [5], Kunii and Smith [6] and Masamune and Smith [7], which represent the heat flow in the bed by a network of gas and solid resistances. The following mechanisms are considered to take place:

† Now at Department of Trade and Industry, Warren Spring Laboratory, Stevenage, Herts, U.K.

‡ Now at Türkiye şişe ve Cam Fabrikalari A.Ş., Istanbul, Turkey.

NOMENCLATURE

- a absorption cross-section per unit volume of bed [m^{-1}]
- b backscattering cross-section per unit volume of bed [m^{-1}]
- B Vortmeyer's layer transmittance
- d_{pi} mean sieve spacing for the ith sieve fraction [m]
- D diffusion coefficient of the gas phase [$m^2 s^{-1}$]
- D_e effective diffusion coefficient of the stagnant packing [$m^2 s^{-1}$]
- D_p mean particle size [m]
- D_{50} median particle size [m]
- D_{84} particle weight fraction at a cumulative weight fraction of 84% [m]
- e particle emissivity
- F deformation factor in the Zehner, and Bauer and Schlünder models
- g_0 distribution for characterizing the particle size distribution in the Bauer and Schlünder model
- h_r radiative heat transfer coefficient [$W m^{-2} K^{-1}$]
- h_{rs} radiative heat transfer coefficient in the gas–solid path [$W m^{-2} K^{-1}$]
- h_{rv} radiative heat transfer coefficient in the gas path [$W m^{-2} K^{-1}$]
- I forward component of radiative flux [$W m^{-2}$]
- l_d mean distance between centres of adjacent particles in direction of heat transfer [m]
- l_g gas film thickness in gas–solid path [m]
- l_s thickness of solid layer in gas–solid path [m]
- k_c conductive component of the effective thermal conductivity [$W m^{-1} K^{-1}$]
- k_e effective thermal conductivity of packed bed [$W m^{-1} K^{-1}$]
- k'_e effective thermal conductivity of gas–solid path [$W m^{-1} K^{-1}$]
- k_g gas thermal conductivity [$W m^{-1} K^{-1}$]
- k_g^* thermal conductivity of gas in a confined space [$W m^{-1} K^{-1}$]
- k_H defined by equation (4) [$W m^{-1} K^{-1}$]
- k_r radiative thermal conductivity [$W m^{-1} K^{-1}$]
- k_s solid thermal conductivity [$W m^{-1} K^{-1}$]
- K backward component of radiative flux [$W m^{-2}$]
- Δm_i weight fraction of the ith sieve fraction
- N number of sieve fractions
- Nu_{rg} radiative Nusselt number based on gas conductivity, $h_r D_p/k_g$
- Nu_{rs} radiation Nusselt number based on solid conductivity, $h_r D_p/k_s$
- q_r radiant flux [$W m^{-2}$]
- Q heat flow [W]
- r radial coordinate [m]
- S cross-sectional area of gas–solid path in Godbee and Ziegler model [m^2]
- T temperature [K]
- x_D effective gas path length in Bauer and Schlünder model [m]
- x_r effective radiation length [m]
- X length of side in Godbee and Ziegler model [m]
- z axial coordinate [m].

Greek symbols

- α Godbee and Ziegler shape factor
- β dimensionless mean particle spacing in the direction of heat transfer, l_d/D_p
- γ Bauer and Schlünder shape factor
- δ area fraction of the solid–solid contact conduction path
- ε bed voidage
- ε_1 gas path area fraction
- ε_2 gas–solid path area fraction
- κ_c ratio of the conductive component of the effective conductivity to the gas conductivity, k_c/k_g
- κ_e ratio of effective bed to gas conductivities, k_e/k_g
- κ_r ratio of the radiative component of the effective conductivity to the gas conductivity, k_r/k_g
- ν ratio of solid to gas conductivities, k_s/k_g
- ξ_1 coefficient of variation of particle size distribution
- σ Stefan–Boltzman constant [$W m^{-2} K^{-4}$]
- ϕ effective gas film thickness in gas–solid path, l_g/D_p
- χ radiation transfer factor
- ψ shape factor derived from Ergun's equation.

(1) conduction through the solid phase;

(2) conduction through the contact surface between neighbouring particles;

(3) radiant transfer between adjacent solid surfaces;

(4) radiant transfer between neighbouring void spaces;

(5) conduction through the gas film near the contact surfaces between adjacent particles;

(6) conduction through the gas in the void spaces.

A general unit cell which illustrates these models is shown in Fig. 1. The heat flow through the cell is divided into three parallel paths. Mechanisms 4 and

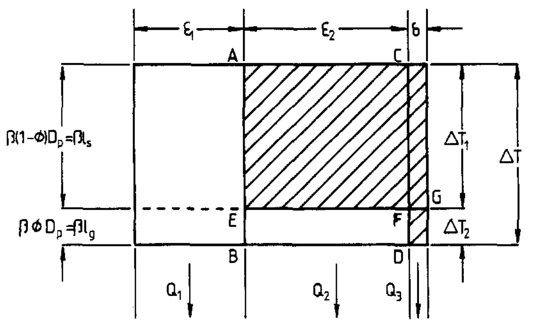

FIG. 1. Unit cell for model of Masamune and Smith [7].

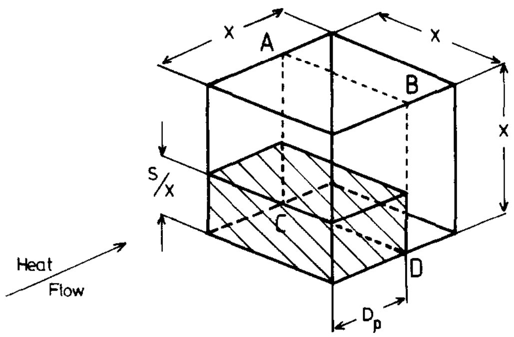

FIG. 2. Unit cell for model of Godbee and Ziegler [8].

6 take place in parallel in the gas path occupying area fraction ε_1. Mechanisms 1, 3 and 5 take place in the gas–solid path occupying area fraction ε_2. Here conduction takes place through the gas and solid in series, with radiant transfer occurring between the solid surfaces. Finally the solid–solid contact conduction path occupies an area fraction δ. The three parallel paths are separated by the adiabatic lines AB and CD: the effective thermal conductivity is then given by

$$\kappa_e = \varepsilon_1\left(1+\frac{h_{rv}\beta D_p}{k_g}\right)+\frac{(1-\varepsilon_1-\delta)}{\dfrac{1-\phi}{\nu}+\dfrac{1}{\dfrac{k_g^*}{\phi k_g}+\dfrac{h_{rs}\beta D_p}{k_g}}}+\nu\delta. \quad (1)$$

Imura and Takegoshi [4] took the two radiant heat transfer coefficients (h_{rs}, h_{rv}) as being equal and derived a theoretical expression for them. They assumed that the mean spacing between particle layers, β, was unity and derived an expression for ε_1, based on the requirement that the unit cell volume fraction was equal to the bed voidage. The model also takes into account the reduction in the gas conductivity at low pressures.

At very low pressures the gas thermal conductivity is very low and the heat flow through the bed is entirely through the contact areas between particles. This allowed the estimation of the solid–solid contact fraction, δ, from conductivity measurements over a range of pressures and the values obtained were very small indicating that at normal pressures, contact conduction makes a negligible contribution to the effective conductivity. They also estimated values of the effective gas film thickness and correlated it against bed voidage, ε, and ν.

2.3. *The Kunii and Smith* [6] *model*

The Kunii and Smith [6] model can also be represented by the general unit cell shown in Fig. 1, with the modifications $\varepsilon_1 = \varepsilon$ and $k_g^* = k_g$. Because no relation had been established between the effective solid and gas thicknesses l_s and l_g and the length of the unit cell, their expression differs from equation (1) by its inclusion of a superfluous parameter in place of the derived term $\beta(1-\phi)$ (which they set equal to 2/3).

The radiant heat transfer coefficients were calculated from expressions derived by Yagi and Kunii [5] and solid–solid contact conduction was considered negligible for atmospheric pressure conditions. Theoretical expressions were derived for the other parameters. They estimated the heat flow in the vicinity of a contact point using a model consisting of two touching spheres. The calculation assumed one-dimensional heat flow with constant linear heat flux through the gas and solid. From a knowledge of the number of contact points per particle effective in transferring heat, they estimated the gas film thickness equivalent to the resistance of the contact points. It should be noted that this effective co-ordination number differs from the true co-ordination number (i.e. the number of contact points per particle) because the heat flow in the region of a contact point depends on its orientation to the overall temperature gradient. A correlation was derived to estimate this parameter.

2.4. *The Godbee and Ziegler* [8] *model*

Godbee and Ziegler [8] expressed the effective thermal conductivity as the sum of three component conductivities representing solid–solid contact conduction, radiation between solid surfaces and conduction through the gas and solid phases. The unit cell for the gas–solid component is shown in Fig. 2 which represents a cubic volume of a bed. It is constructed by redistributing the solid within the cell into a homogeneous block in such a way that the effective conductivity of the cell remains unaltered. The dimensions of the solid section are defined in terms of a shape factor, α, which determines how much of the solid may be considered to be in parallel with the surrounding gas and how much in series. The definition of α is such that the void volume of the cell equals that of the bed. The conductivity of the unit cell is calculated assuming one-dimensional heat transfer but with the isotherms being parallel planes perpendicular to the direction of heat transfer, such as ABCD. The gas–solid component then becomes

$$\frac{k_e'}{k_g}=\frac{1}{\dfrac{D_p/X}{(1-S/X^2)+\nu S/X^2}+(1-D_p/X)}. \quad (2)$$

The shape factor α and the mean particle size are

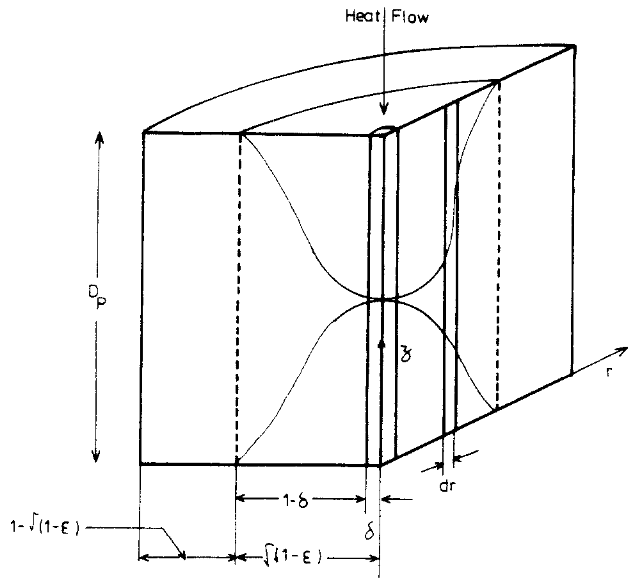

FIG. 3. Unit cell for model of Bauer and Schlünder [11].

calculated from the particle size distribution, assumed log-normal, according to formulae that they give.

2.5. *The Laubitz* [9] *and Russell* [10] *models*

The Russell [10] model also makes the assumption of parallel isotherms in deriving the thermal conductivity of the unit cell. It differs from that of Godbee and Ziegler [8] in that the unit cell consists of a cube of gas containing a cube of solid. The relative dimensions of the cubes are fixed by the requirement that the unit cell voidage equals that of the bed. No provision is made for radiation, solid–solid contact conduction or low pressure effects. Laubitz [9] compared the predictions of the Russell model with measurements taken on beds of magnesia, zirconia and alumina at temperatures up to 1200°C. The predictions were found to be too low, but Laubitz obtained good agreement with some materials by doubling the Russell estimate and adding his own radiation term.

2.6. *The Bauer and Schlünder* [11] *and Zehner* [12] *models*

The Bauer and Schlünder model is an extension of an earlier model by Zehner and Schlünder [12, 13]. Zehner's model is applicable to random packings of uniform spheres and takes into account radiation and pressure effects. The unit cell is shown in Fig. 3. Here again the heat flow is divided into three parallel paths. The first represents conduction and radiation through the gas filled voids and has an area fraction of $1-\sqrt{(1-\varepsilon)}$. The second path represents conduction through the solid and gas phases with radiation between solid surfaces and has an area fraction of $(1-\delta)\sqrt{(1-\varepsilon)}$. Finally, the solid–solid conduction path has an area fraction of $\delta\sqrt{(1-\varepsilon)}$. By paralleling resistances, the effective thermal conductivity becomes

$$\frac{k_e}{k_g} = (1-\sqrt{(1-\varepsilon)})\frac{k_H}{k_g} + \sqrt{(1-\varepsilon)}\left\{(1-\delta)\frac{k_e'}{k_g} + \frac{\delta k_s}{k_g}\right\} \tag{3}$$

with

$$\frac{k_H}{k_g} = \frac{k_g^*}{k_g} + \varepsilon\, Nu_{rg}. \tag{4}$$

Here k_H, the effective conductivity of the void space, is expressed as the sum of a radiative and a conductive component, both of which are dependent on the void space dimensions, taken as εD_p. The gas conductivity in the void space is calculated from an expression by Chapman and Cowling [14] to allow for the influence of pressure. The radiation Nusselt number, Nu_{rg}, is based on an expression by Damköhler [15]. The area fractions have been chosen so that the effective conductivity obeys the limit

$$\lim_{\nu\to 0}\frac{k_e}{k_g} = \frac{D_e}{D} = 1-\sqrt{(1-\varepsilon)}. \tag{5}$$

Zehner [12] considered this expression to represent conduction through a bed of non-conducting particles surrounded by a conducting gas which he considered to be analogous to diffusion in a packed bed and expressed the limit as the ratio of the diffusion coefficient of the stagnant bed, D_e, to that of the gas, D. This ratio can be related to the voidage, ε, by the empirical expression given. The effective thermal conductivity of the gas–solid path is calculated by assuming constant linear heat flux in the z-direction through the gas–solid composite and integrating over the radius to obtain the total heat flow. For this purpose the solid is considered to be bounded by the curve

$$r^2+\frac{z^2}{(F+(F-1)z)^2}=1. \quad (6)$$

The derivation of the gas–solid path conductivity also allows for the influence of pressure on the conductivity of the gas and radiant transfer between the surfaces of the solid phase. In equation (6), F is a deformation factor and is evaluated from the requirement that the void fraction of the unit cell should equal the bed voidage. Approximately

$$F = 1.25\left(\frac{1-\varepsilon}{\varepsilon}\right)^{10/9}. \quad (7)$$

It should be noted that equation (6) is not a representation of the shape of a particle. Zehner extended the model to packings of non-spherical, uniform sized particles by replacing the numerical factor in equation (7) with a shape factor, γ, evaluated for spheres, cylinders and broken solids from numerous experiments.

Bauer extended the Zehner model to deal with random packings of irregular particles with a wide size range. Equation (7) was then rewritten as

$$F = \gamma\left(\frac{1-\varepsilon}{\varepsilon}\right)^{10/9} g_0(\xi_i) \quad (8)$$

where g_0 is a distribution function characterizing the particle size distribution. Bauer and Schlünder [11] measured the effective conductivity of various packings up to 727°C. From experiments on binary mixtures of spheres, they found good agreement was obtained using $\gamma = 1.25$ and the distribution function

$$g_0(\xi_i) = 1+3\xi_1. \quad (9)$$

Here ξ_1 is the coefficient of variation of the particle size distribution and can be calculated from a sieve analysis. For broken solids they found that $\gamma = 1.4$. They also showed that a mean particle size could be used in place of the uniform sphere diameter used in Zehner's model.

2.7. *The treatment of radiation in the unit cell models*

In unit cell models, radiation is treated as a local effect taking place between adjacent particle surfaces and void boundary surfaces in the unit cell. Long range effects are neglected. Vortmeyer [16] lists five assumptions that are made by these models and those considered in the next section:

(1) particle diameter $\gg$ wavelength;
(2) grey emitting surfaces;
(3) opaque solid;
(4) absence of free convection;
(5) $\Delta T/T \ll 1$ across a particle layer.

In these models radiative transfer is considered in terms of either a radiative thermal conductivity or a heat transfer coefficient and usually evaluated by considering the radiant exchange between surfaces in some simplified geometry that is considered to represent best the radiant transfer in the unit cell. Some of the models (e.g. Godbee and Ziegler [8], and Laubitz [9]) calculate the overall effective thermal conductivity by adding the radiative conductivity to the conduction component calculated from the unit cell. Other models (Zehner [12], Bauer and Schlünder [11], Wakao and Kato [1], Imura and Takegoshi [4], and Kunii and Smith [6]) include the radiative conductivity (or heat transfer coefficient) as a resistance in the network of resistances representing the unit cell. In these models where a radiative resistance is considered in series with that of solid conduction, the magnitude of the radiation contribution will depend on the thermal conductivity of the solid [16]. This was demonstrated by Nusselt [17] who considered radiant exchange between slabs of gas and solid in series.

The expressions used to calculate the radiative conductivities for the various models considered are tabulated in Table 1. They are given in the form of a radiative exchange factor, χ, from which the radiative conductivity may be calculated as

$$k_r = 4\sigma\chi D_p T^3. \quad (10)$$

In general χ is a function of the particle surface emissivity and the radiative transfer geometry assumed. The Wakao and Kato [1] expression is based on the consideration of the radiant transfer between touching spheres as shown in Fig. 4. It is assumed that the imaginary surfaces HH′ and II′ circumscribing the spheres are diffusely reflective. In this way they showed that the angle factor between surfaces HI and H′I′ is approximately the same as that between hemispheres AH and AH′, thus allowing the use of a single radiative transfer factor. In this model the interaction between radiation and conduction is complicated, and so the results were presented as a plot of κ_e against v with a radiation Nusselt number Nu_{rs} as a parameter.

The radiant heat transfer coefficient in the Zehner model [12] is based on the Damköhler equation [15] as modified by Argo and Smith [18]. The geometrical configuration consists of two parallel grey planes separated by a particle diameter.

Yagi and Kunii [5] used separate expressions for the radiative heat transfer coefficients through the gas parallel path and the gas–solid path. The gas–solid coefficient is calculated from the Argo and Smith [18] parallel plates expression, whilst that of the gas path is given by their own expression.

In the Imura and Takegoshi model [4], one heat transfer coefficient was used for both parallel paths and calculated from a relationship based on a single radiating plate.

The Godbee and Ziegler model [8] and the Laubitz model [9] both use radiative conductivities that are additive. Both are functions of the voidage as well as the emissivity. The Laubitz expression is based on a consideration of one-dimensional radiant transfer through a void containing solid cubical obstacles. Reflection is neglected in its derivation.

Table 1. Radiation exchange factor for various unit cell models

Authors	χ	Alumina $e = 0.45$ $B = 0.127$	Alumina $e = 1$ $B = 0.095$	Silica $e = 0.37$ $B = 0.097$	Silica $e = 1$ $B = 0.065$
Godbee and Ziegler	$\frac{\varepsilon e}{1-\varepsilon}$	0.528	1.174	0.279	0.754
Laubitz	$\frac{1-(1-\varepsilon)^{2/3}+(1-\varepsilon)^{4/3}}{1-\varepsilon}e$	0.743	1.65	0.51	1.377
Imura and Takegoshi	e	0.45	1.0	0.37	1.0
Wakao and Kato	$\frac{2e}{2-0.264e}$	0.478	1.152	0.388	1.152
Zehner; Bauer and Schlünder	$\frac{e}{2-e}$	0.29	1.0	0.227	1.0
Kunii and Smith	$\frac{1}{\left(1+\frac{\varepsilon}{1-\varepsilon}\frac{1-e}{2e}\right)}$	0.582	1.0	0.609	1.0
Vortmeyer	$\frac{2B+e(1-B)}{2(1-B)-e(1-B)}$	0.478	1.21	0.359	1.14
Kasparek	$\frac{e+B}{1-B}$	0.661	1.21	0.517	1.14

2.8. *The treatment of radiation in pseudohomogeneous models*

Apart from the unit cell models which do not allow for the long range effects of radiation, there are a number of models which consider the bed to be a continuum for radiation and take account of these effects. The bed is considered to be a pseudo-homogeneous medium through which radiation can penetrate freely and is modelled by equations which describe the transfer of radiation through an absorbing, emitting and scattering medium. A derivation of these equations may be found in Özisik [19]. The equations may be written in simplified form as

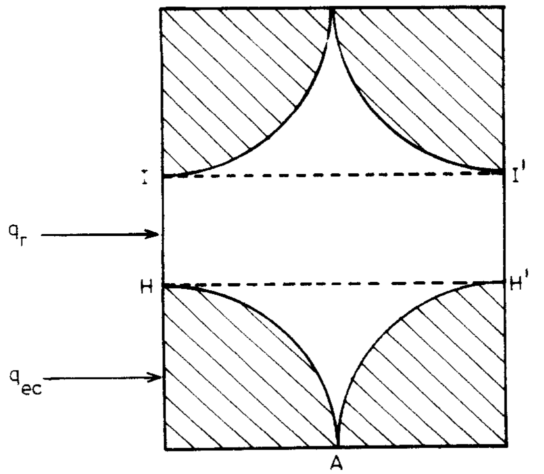

FIG. 4. Wakao and Kato's [1] model for radiation between adjacent particles.

$$\frac{dI}{dz} = -(a+b)I + bK + a\sigma T^4 \tag{11}$$

$$-\frac{dK}{dz} = -(a+b)K + bI + a\sigma T^4. \tag{12}$$

Here it is assumed that the medium is grey, the scattering is isotropic and finally the Schuster–Schwarzchild approximation is applied. This divides the total radiative flux into a forward flux I and a backward flux K, both parallel to the z-axis, hence removing the dependence of the original equations on direction [19]. The net radiative flux may then be written as

$$q_r = I - K.$$

The above equations were first used by Hamaker [20] and have been obtained by Viskanta [21] on simplification of a more rigorous treatment. Since the bed is considered to be homogeneous, there is no direct relationship between the flux parameters and the physical properties of the packing. Churchill and coworkers [22, 23] estimated the effective scattering and absorption parameters b and a by measuring the attenuation of radiation in beds of various packings. Using approximate solutions of equations (11) and (12) subject to boundary conditions, Chen and Churchill [22] derived an expression for the radiant conductivity in the interior of an optically thick bed as

$$k_r = \frac{8\sigma T^3}{a+2b}. \tag{13}$$

This expression was also obtained by Hamaker [20] by a different procedure. Both Chan and Tien [24] and Vortmeyer and Kasparek [25] have established theoretical relationships between continuous and discontinuous models.

Vortmeyer and Kasparek defined a layer transmittance parameter, B, which represented the proportion of radiation transmitted by a single layer. They derived expressions for the flux parameters a and b in terms of particle surface emissivity and B [25]. An expression was also derived for the radiative conductivity and is given in Table 1. This expression is equivalent to equation (13) but with coefficients a and b expressed in terms of Vortmeyer and Kasparek's layer transmittance. Vortmeyer and Börner [26] represented the particle layer as an opaque plate with regularly spaced holes in it and expressed the layer transmittance as a function of emissivity and voidage by considering the radiant exchange between the solid and void surfaces. Kasparek and Vortmeyer [27] introduced a correction to the particle emissivity to take into account reflections between adjacent particles in the same layer and obtained a modified expression for χ (see Table 1).

Vortmeyer and Kasparek [25] considered simultaneous conduction and radiation in a packed bed using a pseudohomogeneous model. They examined the error in the assumption that the overall effective thermal conductivity was the sum of a conductive component and the radiative component calculated from equation (13) and concluded that it was small. Consequently they advise that the radiative conductivities estimated from their models should be added to a conduction component to yield the overall bed effective thermal conductivity.

3. COMPARISON BETWEEN THE EXPERIMENTAL THERMAL CONDUCTIVITY VALUES AND MODEL PREDICTIONS

The experimental measurements for the three bed materials were compared with values predicted by the models of Bauer and Schlünder [11], Zehner [12], Godbee and Ziegler [8], Imura and Takegoshi [4], Wakao and Kato [1], Kunii and Smith [6], Laubitz [9] and Russell [10]. It was difficult to find suitable data for the thermal conductivity and surface emissivity of the solid particles in order to evaluate the models.

3.1. *The thermophysical data used in the model equations*

The alumina used in the experiments (Table 1 of Part I) was 99.7% pure white synthetic α alumina. Touloukian and DeWitt have tabulated thermal conductivity [28] and emittance [29] data from numerous sources for samples of polycrystalline alumina and sapphire. The polycrystalline data seemed more appropriate since polycrystalline alumina is composed of a dense mass of crystals rather like a packed bed, whilst sapphire refers to the single crystal. In addition, it is likely that individual particles in the bed will be composed of more than one crystal. The recommended curve for the thermal conductivity of 99.5% pure, 98% dense polycrystalline alumina was used. The emittance data is considerably scattered because radiative properties are influenced by the condition of the sample used. Touloukian and DeWitt have produced a chart of the normal total emittance of polycrystalline alumina based on an analysis of 23 experimental curves indicating a range of values for each temperature. The values used in the calculations were the midpoints of these ranges.

The sand used in the experiments (Table 1 of Part I) was considered to consist of α quartz below the phase transition temperature of 573°C, and β quartz above. Touloukian and DeWitt [28] have collated thermal conductivity data for crystalline quartz and fused quartz (vitreous or amorphous). The values for crystalline quartz are rather higher than those for fused quartz. Since sand is crystalline, the data for single crystal quartz was used. Crystalline quartz displays a slight degree of anisotropy, its thermal conductivity parallel and perpendicular to the c-axis differing slightly. Calculations were therefore performed with both the perpendicular and parallel conductivities for comparison. Data is only available up to the phase transition temperature. At higher temperatures, extrapolation seems reasonable as the thermal conductivity shows a $k_s \propto 1/T$ dependence as would be expected for an insulating single crystal [30]. Touloukian and DeWitt list only one emittance value for crystalline silica, that of 0.37 taken at 750°C on a sample of α crystobalite. This value was used throughout the temperature range.

The gas in the void spaces of the beds was air, and the thermal conductivity values were taken from those tabulated by Mayhew and Rogers [31]. Some of the conductivity and emittance values used in the calculations are listed in Table 2. As would be expected for a crystalline solid, the conductivity falls with increasing temperature over the range investigated. For alumina, the emittance also falls with increasing temperature.

3.2. *Estimation of the bed parameters*

To evaluate the models it was necessary to estimate certain parameters which characterize the packing of the bed. For the simple models, only the voidage and a mean particle size are required. Except for the Godbee and Ziegler model, the mean size was calculated from the sieve analyses as

$$D_p = \left[\sum_{i=1}^{N} \frac{\Delta m_i}{d_{pi}} \right]^{-1} \tag{14}$$

and is the size used to identify the materials in this work.

For the Godbee and Ziegler model [8] however, the parameters describing the bed were all evaluated from a log probability plot of the sieve size against the

Table 2. Thermophysical property data

T (°C)	Thermal conductivity (W m^{-1} K^{-1}) Alumina	Silica ∥	Silica ⊥r	Air	Emissivity Alumina
977	6.3	2.43	2.08	0.07849	0.45
877	6.75	2.65	2.19	0.07427	0.477
777	7.44	2.91	2.33	0.06985	0.51
677	8.33	3.22	2.49	0.06520	0.552
577	9.58	3.61	2.69	0.06030	0.595
477	11.4	4.1	2.94	0.05509	0.636
377	14.0	4.74	3.26	0.04954	
277	17.75	5.61	3.72	0.04357	

cumulative weight fraction, according to the methods they specify. In this case, the mean particle size is the median, D_{50}, of the distribution. In the case of the Zehner [12] and Bauer and Schlünder models [11], the mean size was calculated from equation (14), but then corrected by a shape factor to yield the gas path and radiation lengths, x_D and x_R, respectively. The shape factors were derived from minimum fluidization velocity measurements using the Ergun [32] correlation. With the exception of the models of Zehner, and Bauer and Schlünder, all the models were evaluated assuming point contacts and also that the pressure was sufficiently high to have no influence on the gas conductivity. For the Zehner, and Bauer and Schlünder models, the contact area was estimated using a method described by Luikov *et al.* [33], but its contribution to the conductivity was found to be negligible. For non-spherical particles, Imura and Takegoshi [4] suggest reducing the estimated gas path length, ϕ, by 10% and so this practice was followed here. The values of the parameters estimated for the Bauer and Schlünder and Godbee and Ziegler models are shown in Table 3. The parameters of the Zehner model are identical to those of the Bauer and Schlünder model except that in evaluating the deformation factor, F, in equation (8), g_0 is taken as unity.

3.3. *Comparison between experimentally estimated and predicted conductivities*

The model predictions are shown together with the experimental values in Figs. 5–7. The silica sand curves were calculated using parallel-axis data. The Wakao and Kato model [1] can only be applied to a bed with voidage close to 0.395 and therefore was not considered appropriate for the alumina bed which had a voidage of 0.54. It is apparent that while all the predictions are of the right order of magnitude, they cover a range of values. Moreover, the temperature dependence of the effective conductivity predicted by the models is generally far less than that determined experimentally. Only the Laubitz model gives good agreement with alumina but this overpredicts for the two grades of silica sand.

4. IMPLICATIONS OF THE EXPERIMENTS AND MODELS

4.1. *The conductive and radiative components of the effective thermal conductivity*

It is useful to consider the effective thermal conductivity to be the sum of a conductive component and a radiative component that is

$$k_e = k_c + k_r. \tag{15}$$

The conditions relating to the validity of this approach have been discussed by Vortmeyer and Kasparek [25]. It is not, however, possible to estimate the value of these components from experimental thermal conductivity measurements without recourse to a model. Nevertheless, by making certain assumptions it is possible to estimate limiting values for the radiative and conductive components. Equation (15) can be

Table 3. Estimated values of the parameters used in the various models

Mean particle size, D_p (μm)	Reference	Alumina 376	Silica 410	Silica 590
Voidage, ε	Godbee and Ziegler [8]	0.54	0.43	0.43
D_{50} (μm)	Godbee and Ziegler [8]	370	447.5	650
D_{84} (μm)	Godbee and Ziegler [8]	425	508	693
Log standard deviation	Godbee and Ziegler [8]	0.1386	0.1268	0.06405
Mean particle size	Godbee and Ziegler [8]	374	451	651
Upper point of truncation (μm)	Godbee and Ziegler [8]	450	567.5	715
Lower point of truncation (μm)	Godbee and Ziegler [8]	330	322.1	465
Shape factor, α	Godbee and Ziegler [8]	0.71	0.96	0.93
Shape factor, ψ	Bauer and Schlünder [11]	0.88	0.9	0.88
x_D	Bauer and Schlünder [11]	427	456	670
x_r	Bauer and Schlünder [11]	427	456	670
Deformation factor, F	Bauer and Schlünder [11]	1.91	3.27	2.94
Contact area fraction, δ	Bauer and Schlünder [11]	9.7×10^{-4}	8.64×10^{-4}	7.84×10^{-4}
Deformation factor, F	Zehner [12]	1.17	1.92	1.90

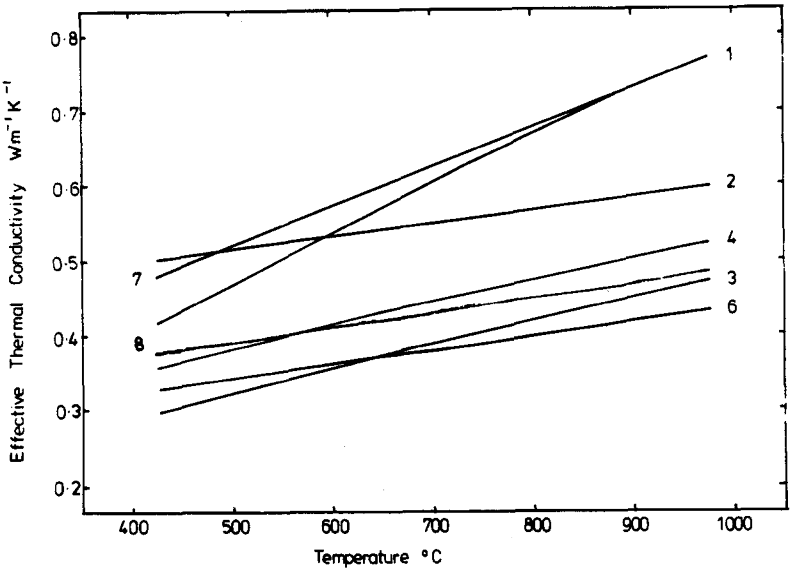

FIG. 5. Comparison between measured effective thermal conductivity of bed of 376 μm alumina and model predictions: 1, experimental; 2, Bauer and Schlünder [11]; 3, Godbee and Ziegler [8]; 4, Imura and Takegoshi [4]; 6, Kunii and Smith [6]; 7, Laubitz [9]; 8, Zehner [12].

made dimensionless by dividing by the gas thermal conductivity

$$\kappa_e = \kappa_c + \kappa_r. \tag{16}$$

Assuming that the conductive component is independent of the radiative component, it can be shown by dimensionless analysis that the dimensionless conduction component, κ_c, for a given bed geometry is a function of the ratio of the solid and gas thermal conductivities, ν. It is evident that κ_c increases monotonically with increasing ν. Figure 8 shows the experimental effective thermal conductivity data for the alumina plotted in dimensionless form. For alumina (and silica) the value of ν falls with increasing temperature which suggests that the value κ_c will fall over the same temperature range. However, Fig. 8 shows that the experimental values of κ_e increase over the temperature range, this rise being entirely due to radiant transfer. Hence, for any observed value of the effective thermal conductivity (e.g. point P on curve AO), the dimensionless radiative component must be larger than the observed increase in κ, that is

$$\kappa_r > \kappa_e - \kappa_o. \tag{17}$$

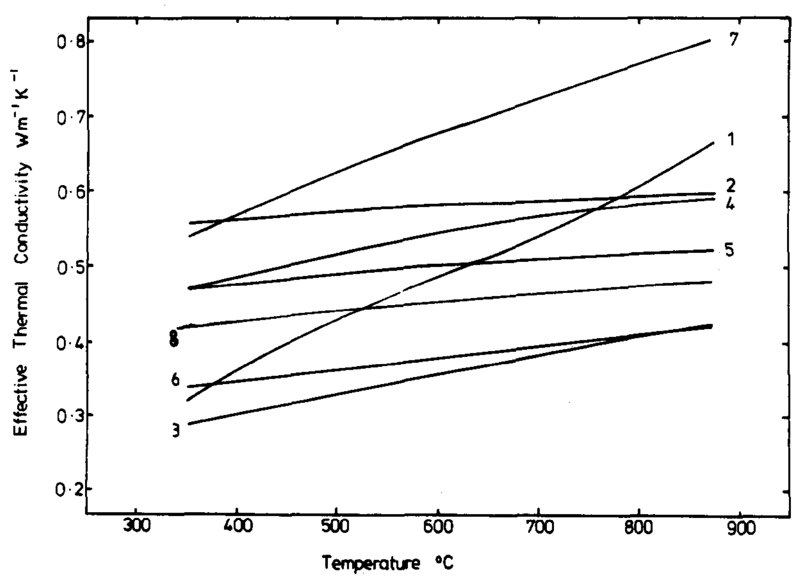

FIG. 6. Comparison between measured effective thermal conductivity of bed of 410 μm silica and model predictions: 1, experimental; 2, Bauer and Schlünder [11]; 3, Godbee and Ziegler [8]; 4, Imura and Takegoshi [4]; 5, Wakao and Kato [1]; 6, Kunii and Smith [6]; 7, Laubitz [9]; 8, Zehner [12].

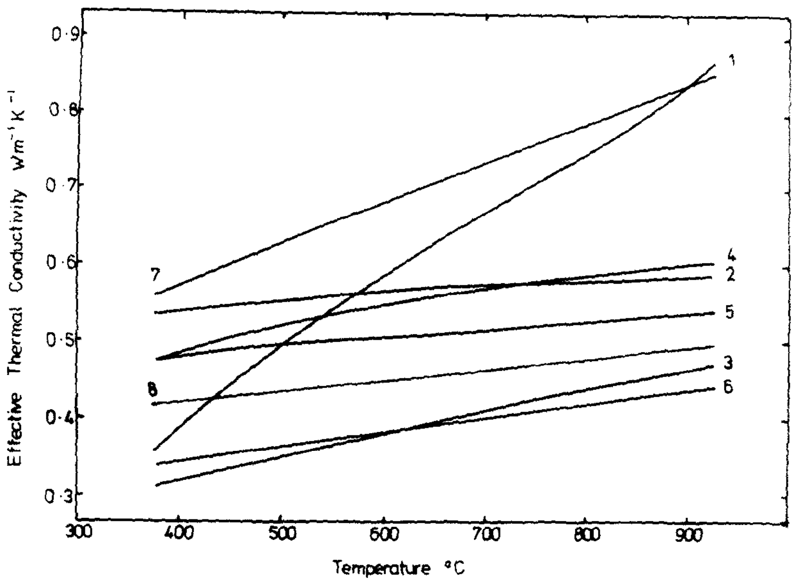

FIG. 7. Comparison between measured effective thermal conductivity of bed of 590 μm silica sand and model predictions: 1, experimental; 2, Bauer and Schlünder [11]; 3, Godbee and Ziegler [8]; 4, Imura and Takegoshi [4]; 5, Wakao and Kato [1]; 6, Kunii and Smith [6]; 7, Laubitz [9]; 8, Zehner [12].

Figure 8 shows that radiation makes a significant contribution to the experimental conductivity, at least 18% at a temperature of 977°C which corresponds to point A. Similar results are obtained for the 410 and 570 μm grades of silica, that is 24.6% at 877°C and 34.5% at 877°C, respectively.

Figure 9 shows the conduction component curves predicted by the models for the silica beds. These were calculated by neglecting the radiation parameters in evaluating the models. The curves in Fig. 9 apply to both the 410 and 590 μm sand because the packings had virtually the same voidage with the consequence that the models, which rely on the voidage to characterize the packing predicted similar values. Also the models which take the particle size distribution into account [8, 11, 12] gave very similar estimates. The models generally yield conductive components with similarly shaped, shallow sloping curves but there is considerable variation between their absolute values. The predictions of the Laubitz model [9] are noticeably higher than the other model predictions and have a curve of steeper slope. This is because they are arbitrarily calculated as twice the value calculated by the Russell model [10]. The Russell curve is shown in Fig. 9 and although the estimates are lower than the rest, it has a slope of similar magnitude. Hence with the exception of the Laubitz model, the models suggest that the conductive component is not greatly influ-

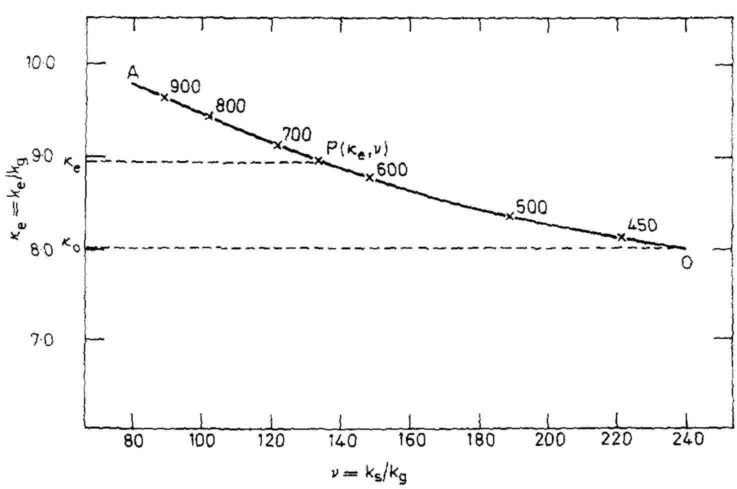

FIG. 8. The experimental effective thermal conductivity of 375 μm alumina in dimensionless form; numbered points refer to corresponding temperatures (°C).

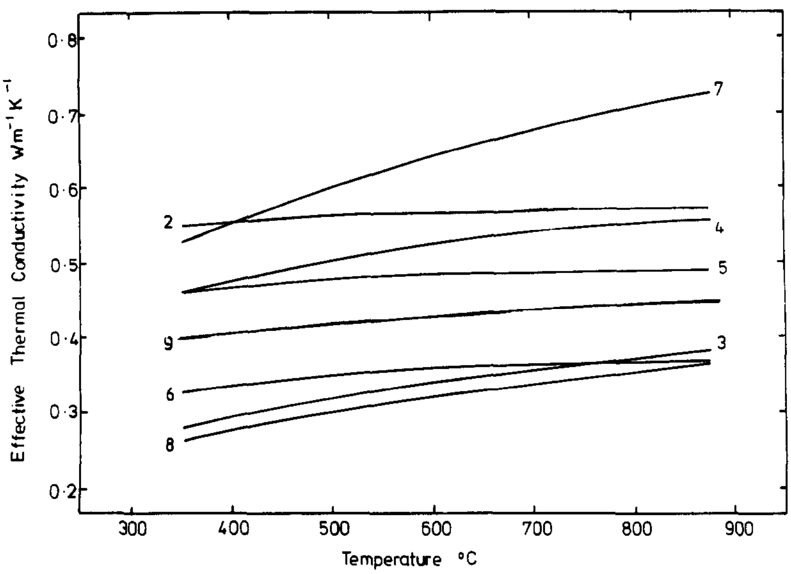

FIG. 9. The conduction component of the effective thermal conductivity of 410 μm silica sand predicted by various models: 2, Bauer and Schlünder [11]; 3, Godbee and Ziegler [8]; 4, Imura and Takegoshi [4]; 5, Wakao and Kato [1]; 6, Kunii and Smith [6]; 7, Laubitz [9]; 8, Russell [10]; 9, Zehner [12].

enced by temperature over the range investigated. Comparison between the conductive component estimates in Fig. 9 and the model estimates in Figs. 6 and 7 shows that the predicted radiative component is small compared with the conductive component. This behaviour of the models is at variance with the deductions made from the experimental data above. Some of the models (Wakao and Kato [1], Imura and Takegoshi [4], Zehner [12], Bauer and Schlünder [11] predict values for the conduction component which are greater than the experimental values at low temperatures. This shows that these models overpredict the conduction component at these temperatures. The Bauer and Schlünder model gives higher predictions than the Zehner model. The main difference between these two models is the allowance for the particle size distribution used in the Bauer and Schlünder model. This function is evidently inapplicable to the narrow size distributions of fine particles used in this work. The Zehner model gives closer predictions of the experimental values and particularly for the alumina.

4.2. *Factors affecting the behaviour of the conductive component*

In Section 3.3 it was pointed out that the conduction component curves of some of the models disagreed with each other and that certain models predicted conduction component curves which were inconsistent with the experimental measurements. However, most of these models have only been tested previously against experimental measurements taken on various packed beds over a limited range of temperatures and have been found to give good results. This would suggest that the overprediction may be due to the failure of these models to deal with beds of materials substantially different to those on which they were originally tested. For example, the correlations of the Imura and Takegoshi models were derived from measurements taken on beds of uniform spheres. In each model, the packing of the bed is characterized by a parameter, which usually corresponds to a dimension in the unit cell and is expressed as a function of various bed properties such as voidage, co-ordination number or particle size distribution. The methods used to evaluate this 'packing parameter', may be empirical or theoretical. For example, the parameter in the Imura and Takegoshi model is derived from an empirical correlation in terms of ε and v. Figure 10 shows the effect of varying this 'packing parameter' on the conductive component predicted by the Imura and Takegoshi models.

The figure shows that for a wide variation in ϕ, the model predicts that the temperature dependence of the conduction component is low compared with that of the experimental results. It was found that all the models exhibited this behaviour when their packing parameters were varied. As these models have been found to give good agreement when fitted to experimental measurements taken at ambient temperature when radiation would be negligible, this suggests that the temperature dependence of the conduction component is indeed low and cannot explain the high temperature dependence of the present experimental results which must therefore be attributed to radiative transfer. Incidentally, two other explanations for the high experimental temperature dependence of the thermal conductivity, namely increasing interparticle contact because of softening at higher temperatures and the development of natural gas convection

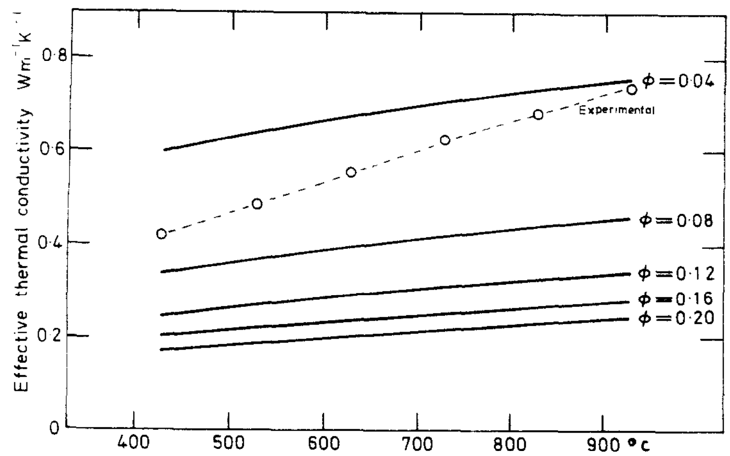

FIG. 10. The effective thermal conductivity of 376 μm alumina predicted by the Imura and Takegoshi model [4] for various values of packing parameter, ϕ.

through the interstices of the bed, were considered and readily discounted [34].

4.3. *Factors affecting the behaviour of the radiative component*

One possible explanation why the models consistently underestimate the degree of temperature dependence is because the emissivity values used in the calculations may not be applicable to the samples of alumina and silica used in the experiments since the emissivity of a material is greatly dependent on the condition of the sample. Consequently, the effect of varying the particle emissivity on the predicted effective thermal conductivity was examined. Figure 11 shows the predicted effective thermal conductivity curves obtained from the Godbee and Ziegler model for the 410 μm sand assuming three possible cases: no radiation at all; the emissivity is given by the reported values; the particles are black ($e = 1$). As the emissivity is increased, the temperature dependence of the model curve increases but even with the maximum emissivity value of unity, the temperature dependence never attains that experimentally observed.

Although there is doubt about the accuracy of the published values for the emissivities of the test materials they would not be as high as one. Whilst surface roughness can considerably increase the effective emissivity of a metallic surface it has only a limited effect on non-metals. This is because radiation is able to penetrate some way below the surface layer of atoms in non-metals before being absorbed or reflected [29]. Consequently it is evident that the models predict a considerably lower radiation contribution than was found.

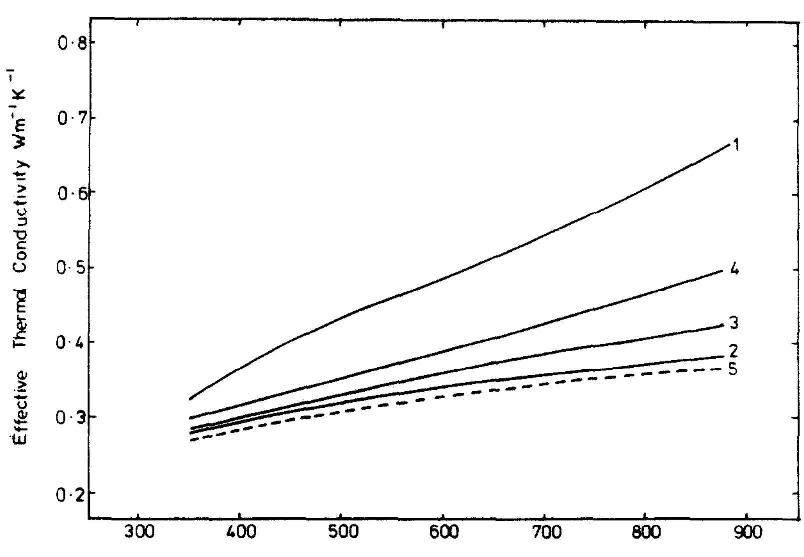

FIG. 11. Comparison between the effective thermal conductivity for a bed of 410 μm silica sand and predictions of the Godbee and Ziegler model [8]; 1, experimental; 2, $e \to 0$; 3, $e \to 0.37$; 4, $e \to 1$; 5, $e \to 0$ and silica conductivity perpendicular to c-axis.

The Godbee and Ziegler model is used to illustrate this point because it gives a conductive component that is consistent with the experimental results and a radiative component which is generally larger than those of the other unit cell models. The radiative components of the different models can be compared by adopting the procedure of Vortmeyer [16] and expressing the various radiative conductivities in the form

$$k_r = 4\sigma\chi D_p T^3. \tag{10}$$

The χ values can then be calculated for each model and compared as in Table 1 in that the higher the value, the higher will be the radiative conductivity. For models where the radiative component is additive (Godbee and Ziegler, Imura and Takegoshi), the radiation component will equal the radiative conductivity given by equation (10) but for the non-additive models the radiative component is less than k_r and dependent on the solid conductivity. Table 1 suggests that only the Laubitz model gives a higher radiative component than that of Godbee and Ziegler. This is because the Laubitz expression neglects reflections between surfaces in its derivation. As noted earlier, Laubitz obtained good agreement with some of the materials he tested by doubling the conduction component predicted by Russell's equation and adding a radiative component. Doubling the conductive component doubles its temperature dependence and as the Laubitz radiation expression gives high results, he was able to reproduce the high temperature dependence of his measurements using reported emissivities. This procedure seems arbitrary and our experiments show that it overpredicts for silica. It follows that if the Godbee and Ziegler model cannot reproduce the temperature dependence of the experimental results then none of the other unit cell models can.

The table also includes the χ values calculated for two pseudohomogeneous models; those of Vortmeyer [16] and Kasparek and Vortmeyer [27] (see Section 2.8). The χ values given by these models are higher than those of the unit cell models but are still not high enough to predict the temperature dependence of the experimental results.

Figure 12 shows the effect of increasing the value of the layer transmittance factor, B, beyond that predicted by Vortmeyer. The calculations were performed using the conductive component predicted by the Godbee and Ziegler model for 410 μm sand and reported emissivities. As B is increased the temperature dependence of the curve increases. At a value of $B = 0.54$ the slope of the model curve is similar to the experimental curve. Also the two curves are roughly coincident suggesting that the estimate of the conductive component is also quite good as well. A similar procedure was adopted for the 376 μm alumina and 590 μm sand giving rise to values for $B = 0.55$ and 0.54, respectively. The χ values for the three beds are 1.62, 1.69 and 1.73, respectively. In the case of alumina, the predicted curve was not coincident with the experimental one as for the 410 μm sand. Consequently the value of B was chosen which produced a curve that was approximately parallel to the experimental one. The justification for this procedure is that it is the temperature dependence (or slope) that should be compared; the discrepancy is due to an underprediction of the conductive component for alumina by the Godbee and Ziegler model. As explained in the previous section, an incorrect prediction of the conductive component has little effect on the overall temperature dependence. The higher estimated values of B are consistent with the transmittance of the bed being far higher than the Vortmeyer model predicts. This is to be expected if the particles are partially transparent to radiation and not opaque as the unit cell and the pseudohomogeneous models assume. Further incidental evidence that this is likely to be so is the fact that heat transfer to fouled boiler tubes is higher than would be accounted for if the deposit were completely opaque to radiation [35].

The considerable transmittance data collated by Touloukian and DeWitt [29] suggests that alumina has a normal spectral transmittance of about 0.8 in the 1–7 μm wavelength range [36] while for silica values of about 0.95 have been observed in the 0.2–4 μm wavelength range [37]. As noted above regarding the values of emissivity for use in the model predictions, there will be similar uncertainty in applying the values of transmissivity to the experimental samples but, using these data, some estimates were made for the normal total transmittances of alumina and silica at 904°C [34]. These estimates assumed a black body distribution; a transmittance of zero for wavelengths where data was unavailable; that the normal spectral transmittance was independent of temperature. The data show that the latter assumption is reasonable for alumina. The calculated normal total transmittances were 0.29–0.36 for 0.254 mm thick samples of polycrystalline alumina and 0.56 for a single crystal sample. For a 1.3 mm thick single crystal of silica, a value of 0.54 was obtained. The two samples of silica gave very similar values of χ and, as they only differ in their particle sizes, this suggests that equation (10) adequately represents the influence of particle size on the radiative component. Although transmittance does decrease with increasing sample thickness, the variation is not marked. For these materials and temperature ranges, the normal total transmittance increases with increasing temperature as the peak of the black body radiation distribution is shifted to the lower wavelengths where alumina and silica are transparent. This increasing transmittance is therefore suggested to be the cause of the strong temperature dependence of the bed's effective conductivity.

5. CONCLUSIONS

Each of the tested models for the prediction of the effective thermal conductivity of static packed beds at temperatures up to 950°C gave a different degree of

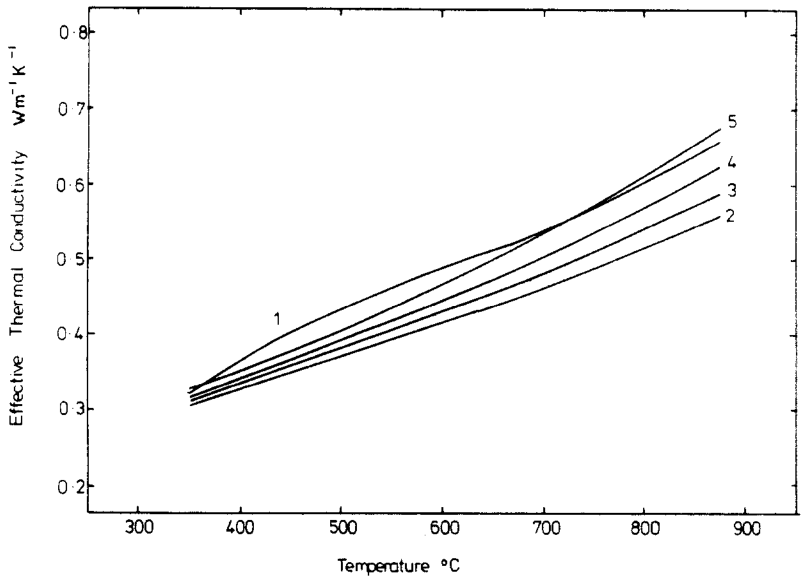

FIG. 12. Estimate of effect of transmittance number, B, for a bed of 410 μm silica sand: 1, experimental; 2, $B = 0.45$; 3, $B = 0.5$; 4, $B = 0.55$; 5, $B = 0.6$.

temperature dependence. Although their predictions were generally within an order of magnitude of measured effective conductivities for beds of 376 μm alumina and 410 and 590 μm silica sand, none could predict the high degree of temperature dependence observed. Their inadequacy is attributed to their treatment of the bed particles as opaque to radiation whereas alumina and silica do transmit certain frequencies.

Deficiencies in the prediction of the conductive component by some models is attributable to their inability to characterize the effects of particle shape and size distribution.

The Godbee and Ziegler [8] and Kunii and Smith [6] models gave reasonable predictions of the conductive component of the silica beds at the lower temperatures for which radiant transfer is negligible.

Acknowledgements—The support of SERC for this work is gratefully acknowledged.

REFERENCES

1. N. Wakao and K. Kato, Effective thermal conductivity of packed beds, *J. Chem. Engng Japan* **2,** 24 (1969).
2. R. G. Deissler and J. S. Boegli, An investigation of effective thermal conductivities of powders in various gases, *Trans. ASME* **80,** 1417 (1958).
3. N. Wakao and D. Vortmeyer, Pressure dependency of effective thermal conductivity of packed beds, *Chem. Engng Sci.* **26,** 1753 (1971).
4. S. Imura and E. Takegoshi, Effect of gas pressure on the effective thermal conductivity of packed beds, *Heat Transfer—Jap. Res.* **3,** 13 (1974).
5. S. Yagi and D. Kunii, Studies on effective thermal conductivities in packed beds, *A.I.Ch.E. Jl* **3,** 373 (1957).
6. D. Kunii and J. M. Smith, Heat transfer characteristics of porous rocks, *A.I.Ch.E. Jl* **6,** 71 (1960).
7. S. Masamune and J. M. Smith, Thermal conductivity of beds of spherical particles, *Ind. Engng Chem. (Fund.)* **2,** 137 (1963).
8. H. W. Godbee and W. T. Ziegler, Thermal conductivities of MgO, Al_2O_3, ZrO_2 powders to 850°C—II. Theoretical, *J. Appl. Phys.* **37,** 55 (1966).
9. M. J. Laubitz, Thermal conductivity of powders, *Can. J. Phys.* **37,** 798 (1959).
10. H. M. Russell, Principles of heat flow in porous insulators, *J. Am. Ceram. Soc.* **18,** 1 (1935).
11. R. Bauer and E. U. Schlünder, Effective radial thermal conductivity of packings in gas flow. Part I. Thermal conductivity of packings in gas flow. Part II. Thermal conductivity of the packing fraction without gas flow, *Int. Chem. Engng* **18,** 189 (1978).
12. P. Zehner, Experimentalle und theoretische Bestimmung der effectiven Wärmeleitfähigkeit durchströmter Kugelschüttungen bei mäßigen und hohen Temperaturen, *VDI Vorschhft.* 558 (1973).
13. P. Zehner und E. U. Schlünder, Wärmeleitfähigkeit von Schüttungen bei mässigen Temperaturen, *Chemie-Ingr-Tech.* **42,** 933 (1970).
14. S. Chapman and T. G. Cowling, *The Mathematical Theory of Non-uniform Gases*, 2nd Edn. Cambridge University Press, Cambridge (1952).
15. G. Damköhler, *Der Chemie Ingenieur* (Edited by Eucken and Jakob), Vol. 3, Part 1, p. 445. Akademischer Verlags—GmbH., Leipzig (1937).
16. D. Vortmeyer, Radiation in packed beds, *Germ. Chem. Engng* **3,** 124 (1980).
17. W. Nusselt, *Z. Bayer. Revis.-Ver.* **17,** 125 (1913).
18. W. B. Argo and J. M. Smith, Heat transfer in packed beds, *Chem. Engng Prog.* **49**(8), 443 (1957).
19. M. N. Özisik, *Radiative Transfer and Interactions with Conduction and Convection*. Wiley, New York (1973).
20. H. C. Hamaker, Radiation and heat conduction in light scattering materials, *Philips Res. Rep.* **2,** 55 and 103 (1947).
21. R. Viskanta, Heat transfer by conduction and radiation in absorbing and scattering materials, *Trans. ASME J. Heat Transfer* **87,** 143 (1965).
22. J. C. Chen and S. W. Churchill, Radiant heat transfer in packed beds, *A.I.Ch.E. Jl* **9,** 35 (1963).
23. B. K. Larkin and S. W. Churchill, Heat transfer by radiation through porous insulations, *A.I.Ch.E. Jl* **5,** 467 (1959).
24. C. K. Chan and C. L. Tien, Radiant transfer in packed spheres, *Trans. ASME J. Heat Transfer* **95,** 302 (1973).

25. D. Vortmeyer and G. Kasparek, Radiative heat transfer in packed beds, J.S.M.E. Semi-Int. Symp. Tokyo, pp. 27–32 (September 1967).
26. D. Vortmeyer und C. J. Börner, Die Strahlungsdurchlasszahl in Schüttungen, *Chemie-Ingr-Tech.* **38**(10), 1077 (1966).
27. G. Kasparek und D. Vortmeyer, Wärmestrahlung in Schüttungen aus Kugeln mit vernachlässigbarem Wärmeleitwiderstand, *Wärme- und Stoffübertr.* **9,** 117 (1976).
28. Y. S. Touloukian and D. P. DeWitt (Editors), *Thermal Conductivity: Non-metallic Solids. T.P.R.C. Data Series—Thermophysical Properties of Matter*, Vol. 1. IFI/Plenum, New York (1970).
29. Y. S. Touloukian and D. P. DeWitt (Editors), *Thermal Radiative Properties of Non-metallic Solids. T.P.R.C. Data Series—Thermophysical Properties of Matter*, Vol. 8. IFI/Plenum, New York (1970).
30. J. E. Parrott and A. D. Stukes, *Thermal Conductivity of Solids*, p. 128. Pion, London (1975).
31. Y. R. Mayhew and G. F. C. Rogers (Editors), *Thermodynamic and Transport Properties of Fluids, S.I. Units*, 2nd Edn. Blackwell, Oxford (1974).
32. S. Ergun, Fluid flow through packed columns, *Chem. Engng Prog.* **48,** 89 (February 1952).
33. A. V. Luikov, A. G. Shaskov, L. L. Vasiliev and Yu. E. Fraimin, Thermal conductivity of porous systems, *Int. J. Heat Mass Transfer* **11,** 117 (1968).
34. A. G. Salway, The effective thermal conductivity of high temperature, particulate beds, Ph.D. thesis, University of Birmingham (1983).
35. B. J. Gliddon, Private communication (1983).
36. R. C. Folweiler, Thermal radiation characteristics of transparent and translucent materials under non-isothermal conditions, U.S.A.F., ASD-TDR-62-719, pp. 1–115 (1961).
37. N. W. Coblentz, Infra-red absorption and reflection spectra, *Phys. Rev.* **23,** 125 (1906).

CONDUCTIVITE THERMIQUE EFFECTIVE DES LITS PARTICULAIRES A HAUTE TEMPERATURE—II. PREDICTIONS DES MODELES ET VALEURS EXPERIMENTALES

Résumé—On passe en revue plusieurs modèles connus, du type à la fois cellule unitaire et pseudohomogène, pour illustrer les approches différentes dans la modélisation de la conductivité thermique effective. Leurs prédictions sont comparées avec des valeurs expérimentales obtenues pour des lits fixes d'alumine et de sable, dans le domaine de température de 400 à 950°C. Aucun modèle ne prédit convenablement aux températures élevées. Ceci est attribué à l'hypothèse que les particules sont opaques au rayonnement tandis que l'alumine et la silice sont semi-transparentes. Les déficiences de quelques modèles sont atribuées à l'inaptitude à caractériser les effets de la forme de la particule et de la distribution en taille. Les modèles de Godbee at Ziegler (*J. Appl. Phys.* **37**, 55 (1966)) et Kunii et Smith (*A.I.Ch.E. Jl* **6**, 71 (1960)) donnet des previsions raisonnables pour la composante conductive des lits de silice aux températures faibles pour lesquelles le transfert radiatif est négligeable.

DIE EFFEKTIVE WÄRMELEITFÄHIGKEIT VON SCHÜTTUNGEN BEI HOHEN TEMPERATUREN—II. MODELL

Zusammenfassung—Es wird ein Überblick über veröffentlichte Modelle—sowohl von Einheitszellen als auch Pseudohomogenität ausgehend—gegeben, um die unterschiedlichen Möglichkeiten zur Modellierung der effektiven Wärmeleitfähigkeit zu illustrieren. Daraus resultierende Werte werden mit denen verglichen, die für Schüttungen von Aluminium bzw. Sand im Temperaturbereich von 400 bis 950°C experimentell bestimmt wurden. Keines der Modelle beschreibt die beobachtete hohe Temperaturabhängigkeit. Die Ursache für dieses Unvermögen wird darin vermutet, daß die Partikel als opak angenommen werden, während sowohl Aluminium als auch Silizium teilweise transparent sind. Mängel einiger Modelle in der Beschreibung der leitenden Komponente werden der Unfähigkeit zur Berücksichtigung des Einflusses von Partikelform und -größenverteilung zugeschrieben. Die Modelle von Godbee und Ziegler (*J. Appl. Phys.* **37**, 55 (1966)) und Kunii und Smith (*A.I.Ch.E. Jl* **6**, 71 (1960)) lieferten eine brauchbare Beschreibung der leitenden Komponente von Sandschüttungen bei tieferen Temperaturen, wo der Strahlungsanteil vernachlässigbar ist.